Table S1 – RNAi lines tested

Gene	Available Lines	Germline mRNA depletion achieved	Observed phenotype
CG5003	v26680	80%	Early embryonic arrest or delay
	v26679	65%	n.p.*
	BL51408	75%	n.p.
	BL31061	n.d.^	n.p.
	BL51403	n.d.	n.p.
Tsp97E	v109600	95%	n.p.
	v4391	95%	n.p.
CG6966	v105934	65%	n.p.
	BL51409	95%	Low penetrance mitotic defect
CG14230	BL51412	93%	Abnormal nurse cell number
stim	v47073	n/a	n.p.
CG30377	BL51386	n.d.	n.p.
CG14516	BL35802	65%	n.p.
CBP	v5680	n.d.	n.p.
	v104064	n.d.	n.p.
TotC	v14420	40%	n.p.
	v106379	55%	n.p.
	BL51407	n.d.	n.p.
CG8188	v103362	85%	n.p.
CG4991	v108419	n.d.	n.p.
	BL44450	80%	n.p.
Nahoda	v102319	n.d.	n.p.
	BL51683	n.d.	n.p.
Itp-r83A	v6484	n.d.	n.p.
	BL51686	50%	n.p.
Rca1	BL51680	n.d.	n.p.
	BL51450	n.d.	n.p.
CG7730	BL36851	98%	n.p.
Fur2	BL51743	92%	n.p.
	BL42577	80%	n.p.
CG11151	BL51413	97%	n.p.
CG17018	BL57024	n.d.	n.p.
Crag	BL33594	n.d.	n.p.
CAH2	BL41836	44%	n.p.
lin19	BL36601	94%	n.p.

kdm4A	BL34629	n/a	n.p.
RAF2	BL34395	94%	n.p.
pzg	BL35448	75%	n.p.
CG17528	BL26292	9%	n.p.
	BL51404	55%	n.p.
CG7840	BL34954	n/a	n.p.
	BL32379	7%	n.p.
NaPi-III	BL29408	90%	Abnormal embryonic divisions
CG7627	BL32337	38%	n.p.
	BL51679	23%	n.p.
CG4476	BL38930	n.d.	n.p.
M1BP	BL32858	60%	n.p.
CG10254	BL51687	n.d.	n.p.
	v108657	n.d.	n.p.
mod(mdg4)	BL33907	n.d.	Abnormal embryonic divisions
	BL32995	n.d.	Abnormal embryonic divisions
CG6962	BL51682	98%	n.p.
CG6927	BL51684	90%	Low penetrance mitotic defect
	BL42001	n.d.	n.p.
CG7777	BL44464	50%	n.p.
	BL50695	50%	n.p.
fzr2	BL38223	88%	n.p.
CG2924	v104482	n.d.	n.p.
sip2	BL33691	n.d.	n.p.
tlk	BL35298	63%	n.p.
ATPalpha	BL32913	n.d.	n.p.
	BL33646	n.d.	n.p.
	BL51411	n.d.	n.p.
mCherry	BL35785	-	-

*No observable phenotype (n.p.)
^No data (n.d.)

Table S2 – Transposable element insertion lines tested

Gene	Tested lines	Associated allele	Observed phenotype
CG5003	BL18566	*CG5003*$_{f02616}$	Early embryonic arrest or delay
	BL22065	*CG5003*$_{DP01070}$	
Tsp97E	BL37653	*Tsp97E*$_{MI04380}$	n.p.*
CG30377	BL19152	*CG30377*$_{d00826}$	Eggs not fertilized
	BL30598	*CG30377*$_{MI00023}$	
	BL43832	*CG30377*$_{MI07499}$	
CG17734	BL19856	*CG17734*$_{EY06693}$	n.p.
CG4586	BL18419	*CG4586*$_{f01234}$	n.p.
CG4991	BL24186	*CG4991*$_{MB03239}$	n.p.
Rca1	BL9162	*Rca1*$_{IX}$	Low penetrance embryonic phenotype
	BL11294	*Rca1*$_{03300}$	
Fur2	BL11429	*Fur2*$_{EP1493}$	n.p.
	BL57092	*Fur2*$_{A}$	
koko	BL6962	*koko*$_{ED2}$	n.p.
	BL21798	*koko*$_{DP00113}$	
yin	BL32630	*yin*$_{G10332}$	n.p.
	BL19172	*yin*$_{d02176}$	
CG15570	BL43789	*CG15570*$_{MI06763}$	Abnormal nurse cell number
WRNexo	BL18267	*WRNexo*$_{e04496}$	n.p.
Fas1	BL36987	*Fas1*$_{MI03699}$	n.p.
	BL21537	*Fas1*$_{DG16410}$	
	BL19855	*Fas1*$_{EY0662}$	
CG17018	BL57930	*CG17018*$_{MI12332}$	n.p.
CAH2	BL42463	*CAH2*$_{MI07079}$	Early embryonic arrest or delay
	BL25562	*CAH2*$_{MB07616}$	
cue	BL24077	*cue*$_{MB03598}$	n.p.
	BL655	*cue*$_{2}$	
	BL15336	*cue*$_{EY01263}$	
mei-P26	BL25717	*mei-P26*$_{mfs2}$	Arrest in early oogenesis
	BL25919	*mei-P26*$_{mfs1}$	
CG6178	BL13992	*CG6178*$_{KG05318}$	n.p.
	BL17104	*CG6178*$_{EP3251}$	
	BL17388	*CG6178*$_{EY0763}$	
CG15721	BL25490	*CG15721*$_{MB06259}$	n.p.
	BL18718	*CG15721*$_{f03962}$	

NaPi-III	BL24722	*NaPi-III*$_{MB04559}$	Abnormal embryonic divisions
CG7627	BL18426	*CG7627*$_{f01338}$	n.p.
CG4476	BL19350	*CG4479*$_{d11470}$	Low penetrance embryonic arrest or delay
	BL30944	*CG4476*$_{MI00100}$	
CG10960	BL37000	*CG10960*$_{MI03549}$	Abnormal embryonic divisions
	BL24047	*CG10960*$_{MB03129}$	

*No observable phenotype (n.p.)

Table S3 – Glycogen pathway enzyme gene RNAi lines tested

Gene	RNAi lines Tested
Trehalase (Treh)	BL50585
Hexokinase C (HK)	BL57404
Phosphoglucosemutase (Pgm)	BL34345
UTP--glucose-1-phosphate uridylyltransferase (UGP)	BL50902
	BL52968
Glycogenin	BL42565
Glycogen synthase (GlyS)	BL34930
	BL50956
1,4-Alpha-Glucan Branching Enzyme (AGBE)	BL40860
	BL42753
Glycogen phosphorylase (GlyP)	BL33634

A

nebu RNAi

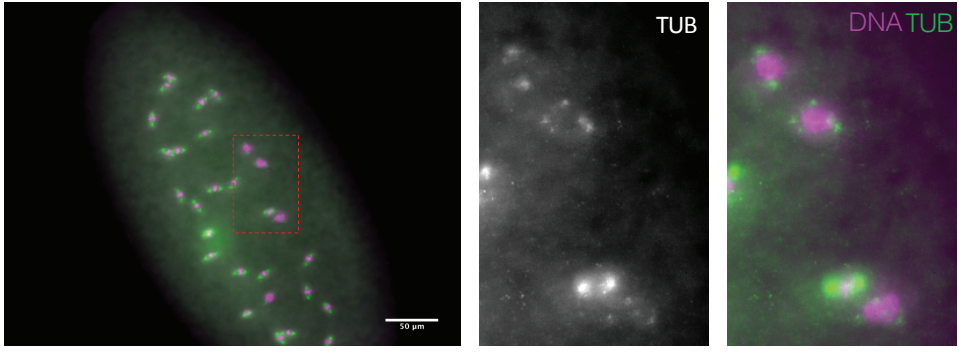

B

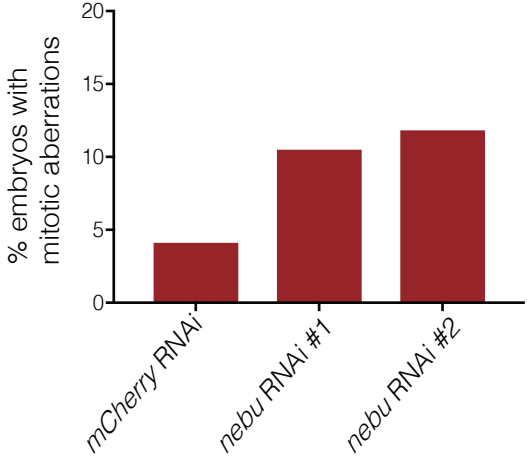

C

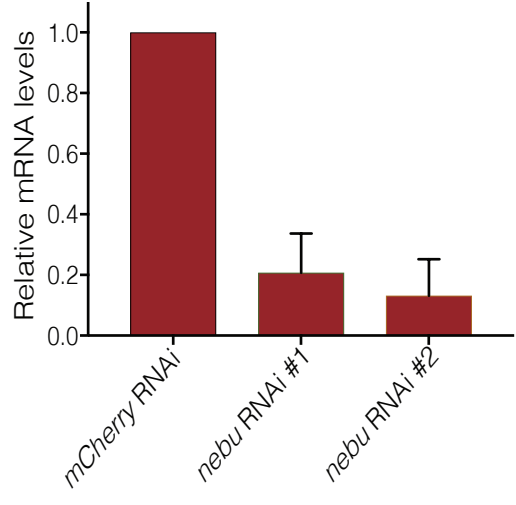

Figure S1. *nebu* RNAi recapitulates the *nebu* mutant embryonic phenotype. RNAi against *nebu* was driven during late oogenesis using a *matα-GAL4* driver, also driving expression of *UAS-Dicer2*. (A) Defects in mitosis were observed in *nebu* RNAi embryos; multipolar spindles and seemingly polyploid nuclei (insets) were present as in embryos from mothers with the transposon insertion alleles of *nebu*. DNA is shown in magenta, and anti-tubulin is shown in green. (B) Embryos from two different *nebu* RNAi lines exhibit mitotic defects (10.5% and 11.9%, respectively), whereas only 4.2% of a *mCherry* RNAi control showed mitotic defects. The difference between the observed phenotypic frequency in *nebu* RNAi and control was significant (Binomial test, $p < 0.0001$). (C) Q-PCR analysis of mature oocyte samples shows depletion of *nebu* mRNA in *nebu* RNAi lines relative to an *mCherry* control, with greater than 75% of total *nebu* mRNA being depleted in both lines (mRNA reduced to 20.7±12.9% of control for *nebu* RNAi #1 and 13.1±12.10% for *nebu* RNAi #2).

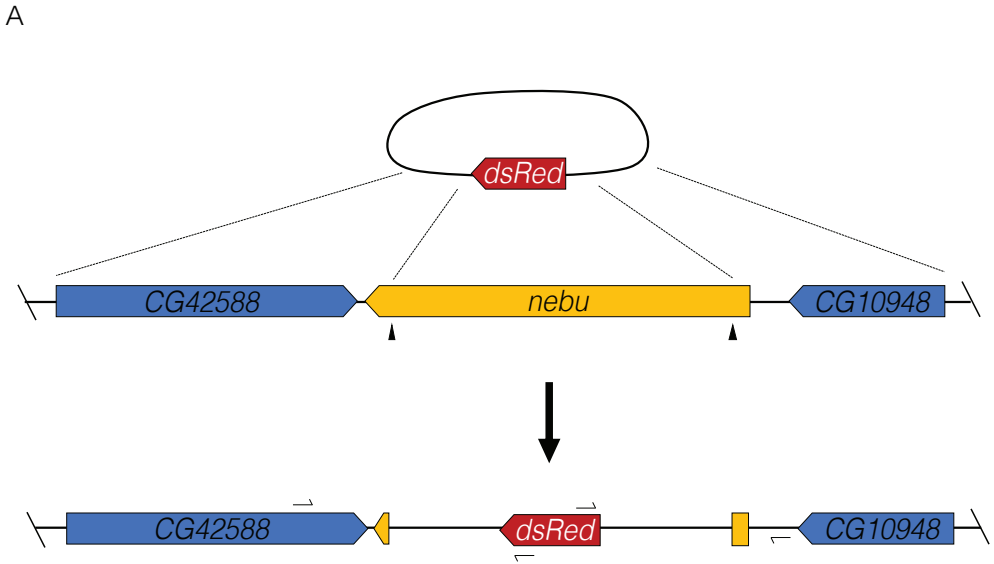
A
dsRed
CG42588
nebu
CG10948
CG42588
dsRed
CG10948

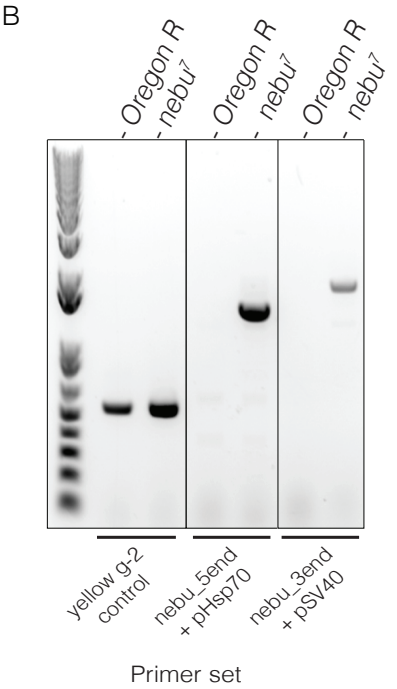
B
Oregon R
nebu7
Oregon R
nebu7
Oregon R
nebu7
yellow g-2 control
nebu_5end + pHsp70
nebu_3end + pSV40
Primer set

Figure S2. Generation of a *nebu* null allele by CRISPR-mediated deletion. (A) *nebu* CRISPR deletion strategy. We generated gRNAs targeting the ends of the *nebu* locus. To induce homology-directed repair, we co-injected the gRNA plasmids with a donor plasmid carrying a *dsRED* marker and two homology arms to the regions immediately outside the gRNA target sites. (B) PCR confirmation of *nebu* CRISPR deletion. Primers sets used were designed to span the junction between the *dsRED* marker and the flanking genomic region.

A

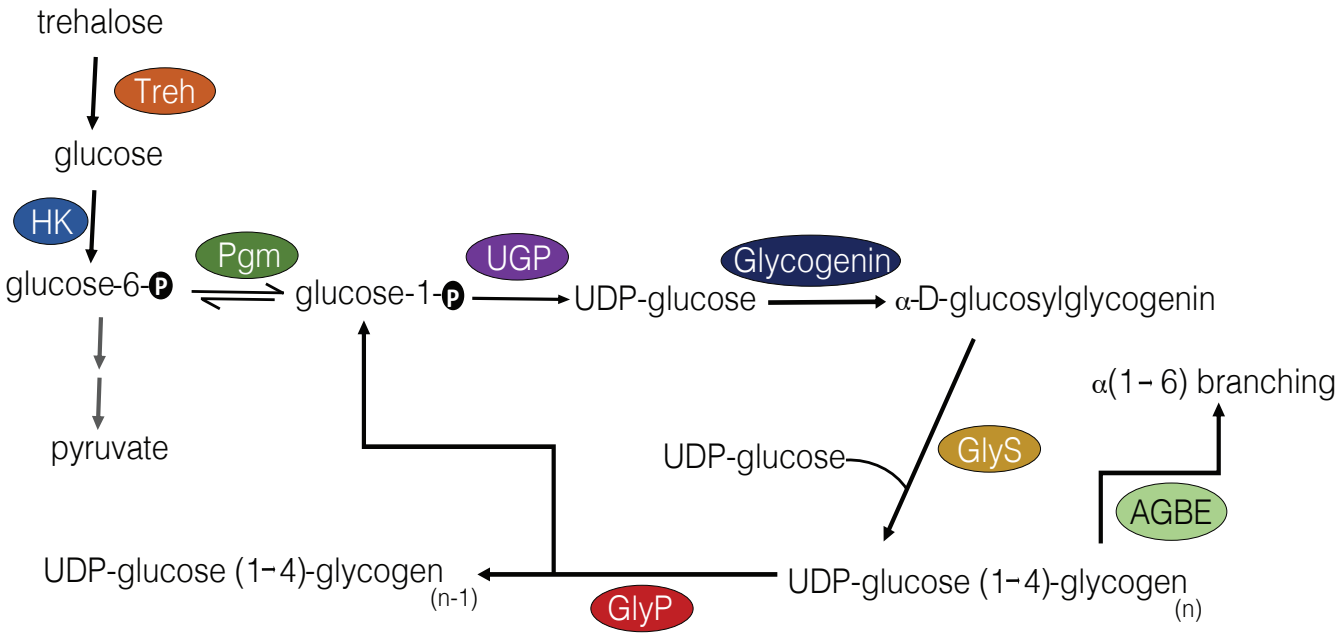
trehalose
Treh
glucose
HK
glucose-6-P
Pgm
glucose-1-P
UGP
UDP-glucose
Glycogenin
α-D-glucosylglycogenin
pyruvate
UDP-glucose
GlyS
α(1−6) branching
AGBE
UDP-glucose (1−4)-glycogen (n-1)
GlyP
UDP-glucose (1−4)-glycogen (n)

B

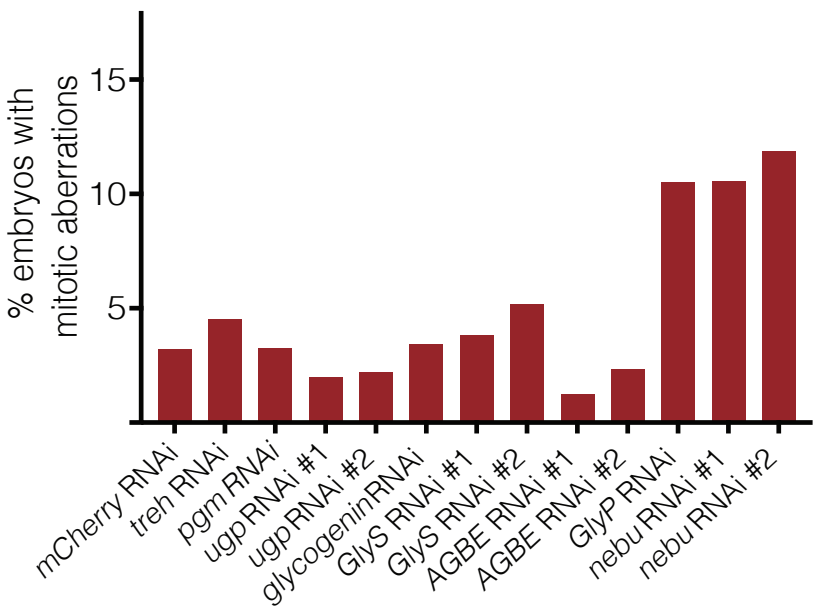
% embryos with mitotic aberrations
15
10
5
mCherry RNAi
treh RNAi
pgm RNAi
ugp RNAi #1
ugp RNAi #2
glycogenin RNAi
GlyS RNAi #1
GlyS RNAi #2
AGBE RNAi #1
AGBE RNAi #2
GlyP RNAi
nebu RNAi #1
nebu RNAi #2

Figure S3. Disruption of glycogen metabolic enzyme leads to mitotic defects in early embryogenesis. (A) Schematic of the glycogen metabolic pathway. Once glucose is converted into glucose-6-phosphate by hexokinase C (HK), it can enter glycolysis and produce pyruvate, or it can be converted into glucose-1-phosphate by phosphoglucomutase (Pgm). UTP-glucose-1-phosphate uridylyltransferase (UGP) converts glucose-1-phosphate into UDP-glucose, which is then used by glycogenin to produce α-D-glucosylglycogenin, which is used by glycogen synthase (GlyS) to kick start glycogen production. GlyS then produces UDP-glucose α(1→4)-glycogenin (linear glycogen) by subsequent addition of UDP-glucose monomers. Branching in the glycogen polymer can be catalyzed by 1,4-alpha-glucan branching enzyme (AGBE) which produces α(1→6) branching. Glycogen phosphorylase is the main catalytic enzyme in glycogen breakdown, catalyzing the production of glucose-1-phosphate from a glycogen polymer. The released glucose-1-phosphate can be either reused for glycogen synthesis or feed into glycolysis. (B) Quantification of embryonic phenotype in knockdown of glycogen metabolic enzymes. RNAi against different enzymes of the glycogen pathway was driven with *matα-GAL4* germline driver, also driving expression of *UAS-Dicer2*, and 2-hour embryos were collected, fixed and stained for DNA and tubulin. The fraction of embryos with mitotic defects are shown out of the total number of collected, and mitotic defects refer to arrested or delayed mitoses, and multipolar spindles. *GlyP* RNAi embryos exhibited mitotic phenotypes at a significantly different frequency than in the *mCherry* RNAi control (Binomial test, $p < 0.0001$), and was comparable to the frequency observed in *nebu* RNAi.

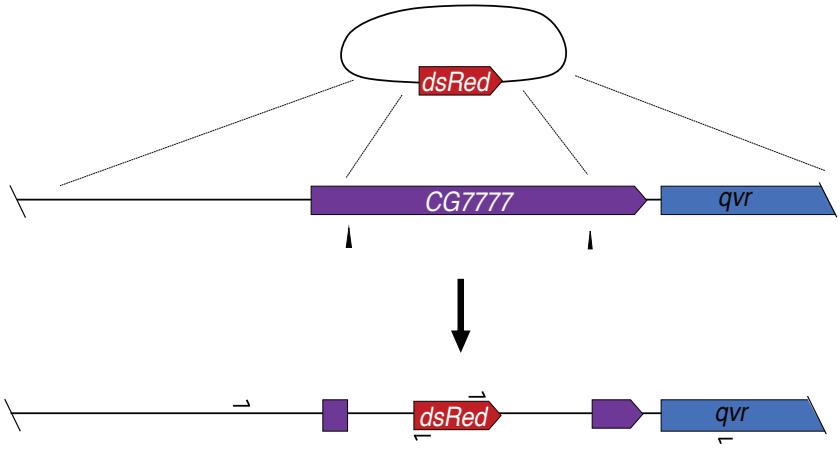
A
dsRed
CG7777
qvr
dsRed
qvr

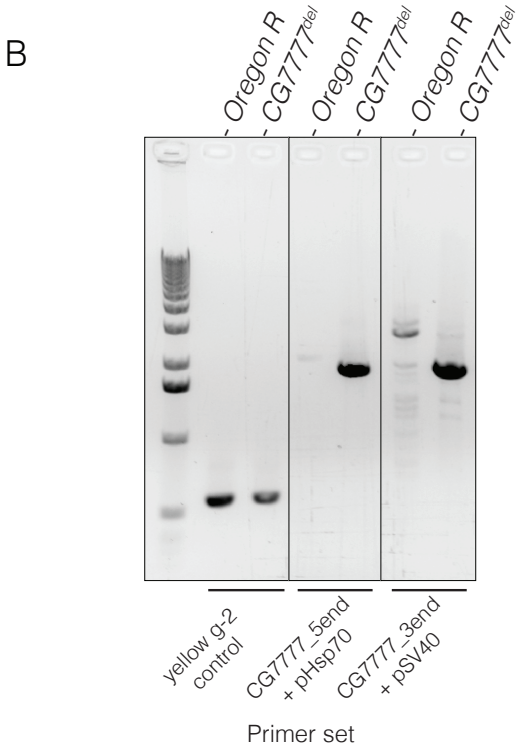
B
Oregon R
CG7777del
Oregon R
CG7777del
Oregon R
CG7777del
yellow g-2 control
CG7777_5end + pHsp70
CG7777_3end + pSV40
Primer set

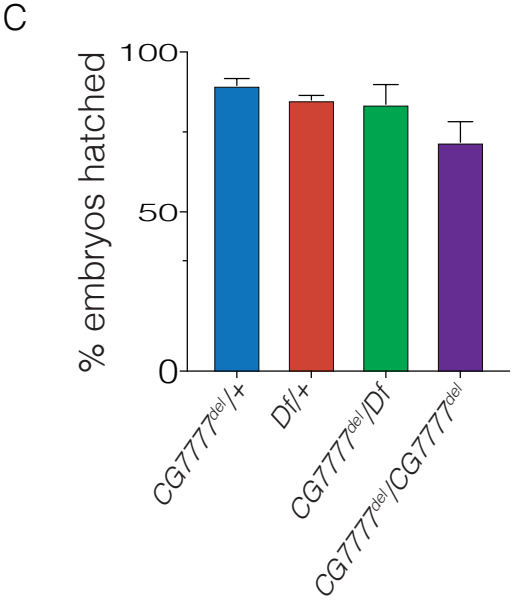
C
% embryos hatched
100
50
0
CG7777del/+
Df/+
CG7777del/Df
CG7777del/CG7777del

Figure S4. CG7777 is dispensable for female fertility. (A) CRISPR deletion of *CG7777*. We generated gRNAs targeting the ends of the *CG7777* locus. To induce homology-directed repair, we co-injected the gRNA plasmids with a donor plasmid carrying a *dsRED* marker and two homology arms to the regions immediately outside the gRNA target sites. (B) PCR confirmation of *CG7777* CRISPR deletion. Primers sets used were designed to span the junction between the *dsRED* marker and the flanking genomic region. (C) Hatching assay analysis of eggs laid by *CG7777* null females. Only the difference between $CG7777_{del}$/ $CG7777_{del}$ and $CG7777_{del}$/+ is significant (two-tailed t-test, $p < 0.05$).